

identical with

$$\{[m^x(\mathbf{p})]^{-1} - \mathcal{K}(\mathbf{p}) + \mathcal{K}'(\mathbf{p})\}_{\mathbf{p} \rightarrow 0} = 0. \quad (\text{V.202})$$

On the other hand, from (V.77),

$$[\mathfrak{M}'(\mathbf{p})/\mathfrak{M}(\mathbf{p})] = \mathcal{K}'(\mathbf{p})\{[m^x(\mathbf{p})]^{-1} - \mathcal{K}(\mathbf{p})\}^{-1}, \quad (\text{V.203})$$

and

$$\mathfrak{M}^{-1}(\mathbf{p}) = \{[m^x(\mathbf{p})]^{-1} - \mathcal{K}(\mathbf{p})\} - \{[m^x(\mathbf{p})]^{-1} - \mathcal{K}(\mathbf{p})\}^{-1}[\mathcal{K}'(\mathbf{p})]^2. \quad (\text{V.204})$$

Combining (V.202), (V.203), and (V.204), we complete the proof for Theorem 3.

## Calculations of Total Cross Sections for Scattering from Coulomb Potentials with Exponential Screening\*

G. H. LANE† AND E. EVERHART

*Physics Department, University of Connecticut, Storrs, Connecticut*

(Received September 10, 1959)

Momentum transfer cross sections and total cross sections are calculated for scattering from the potential energy function  $V = (Z_1 Z_2 e^2/r) \exp(-r/a)$ . Here the first factor is the Coulomb term and the exponential factor contains a screening length  $a$ . The cross sections are obtained by integrating the differential cross section over all angles using a classical calculation or a Born approximation calculation according to whichever is valid. The validity criteria are discussed as they depend on the de Broglie wavelength of the scattered particle. In certain cases the Born approximation solution is valid at small angles and the classical solution is valid at large angles. Graphs and tables are presented showing the results as functions of suitable parameters.

The momentum transfer cross section is finite in all cases and the total cross section is finite except in the classical limit. In this limit, however, calculations are presented showing that portion of the total cross section which arises from scattering through angles greater than a specified small angle.

### 1. INTRODUCTION

THE screened Coulomb potential energy function is often used to describe the interaction between two colliding atoms. It is useful in an energy range extending from a few hundred electron volts to several hundred thousand electron volts. The function under consideration is

$$V = (Z_1 Z_2 e^2/r) \exp(-r/a), \quad (1)$$

where  $Z_1 e$  and  $Z_2 e$  are the nuclear charges of the colliding atoms and  $a$  is a screening length. Differential cross sections were computed classically for scattering from this potential energy function in a paper,<sup>1</sup> hereinafter called reference I, and similar calculations which agree well have been made by Firsov.<sup>2</sup> Experimental measurements of differential cross section for ion-atom collisions by Fuls *et al.*<sup>3</sup> agree very well with the calculated values. Evidently one may use the classical calculations of I with some confidence to obtain values of impact parameter and distance of closest approach, as well as

differential cross section at various scattering angles. It was, therefore, thought desirable to extend the calculations to obtain certain total scattering cross sections for this potential.

It has long been recognized that the Coulomb potential gives rise to an infinite total cross section both classically and quantum mechanically. The addition of the exponential screening factor, however, makes this total cross section finite except in the purely classical limit, as seen in the values to be presented in Sec. 4 below.

Although the total elastic scattering cross section is a well-established concept, it is not particularly useful because it cannot be measured. The reason, of course, is that extremely gentle collisions make up a large part of the total cross section, and one cannot experimentally tell the difference between an unscattered particle and one which has been scattered through a minute angle. One way of avoiding this difficulty is to calculate, as in Sec. 5 below, only that portion of the total cross section which results from scattering in excess of a specified angle.

Perhaps a more useful cross section is that for momentum transfer. This incorporates a  $1 - \cos\theta$  factor in the integrand, which gives a low weight to the gentle forward collisions and a proportionally higher weight to the more violent collisions. The momentum transfer cross section enters into calculation of diffusion coeffi-

\* This work was sponsored by the Office of Ordnance Research, U. S. Army, through the Ordnance Materials Research Office at Watertown and the Boston Ordnance District.

† Now at Franklin and Marshall College, Lancaster, Pennsylvania.

<sup>1</sup> E. Everhart, G. Stone, and R. Carbone, *Phys. Rev.* **99**, 1287 (1955). Hereinafter called reference I.

<sup>2</sup> O. B. Firsov, *J. Exptl. Theoret. Phys. (U.S.S.R.)* **34**, 447 (1958) [*Soviet Phys. JETP* **7**, 308 (1958)].

<sup>3</sup> E. N. Fuls, P. R. Jones, F. P. Ziemba, and E. Everhart, *Phys. Rev.* **107**, 704 (1957).

cients as discussed by Massey and Burhop.<sup>4</sup> This quantity is calculated in Sec. 3 below and it is seen that the momentum transfer cross section is finite in all cases including the purely classical limit.

The general procedure in calculating total cross section is to integrate the differential cross section over all angles. No exact solution for differential cross section is known for this potential. In addition to the classical calculations of I, there is the well-known solution by the Born approximation method. Generally speaking, these two solutions are valid in mutually exclusive regions and it will be necessary to examine carefully the respective validity criteria. In certain cases the integration must be carried across an angular region where neither of the above solutions for differential cross section are strictly valid, and the calculation gives approximate values which are uncertain, perhaps to within a factor of two. In other cases the difficult angular region does not contribute significantly and the results are accurate. All calculations are made in center-of-mass coordinates.

## 2. VALIDITY CRITERIA

There are three characteristic lengths which appear as parameters in the solution. The first of these, the screening length  $a$  of Eq. (1), is often taken<sup>5</sup> to be

$$a = a_0 / [Z_1^{\frac{1}{2}} + Z_2^{\frac{1}{2}}]^{\frac{1}{2}}, \quad (2)$$

where  $a_0 = 0.53 \times 10^{-8}$  cm.

The second of these lengths is a parameter  $b$  defined by

$$b = Z_1 Z_2 e^2 / (\frac{1}{2} m v^2), \quad (3)$$

where  $m$  is the reduced mass and  $v$  is the relative velocity of the atoms before collisions. In the absence of screening, as in Rutherford scattering,  $b$  would be termed the collision diameter.

The third characteristic length is  $\lambda$ , the de Broglie wavelength, given by

$$\lambda = \hbar / m v. \quad (4)$$

Discussions of the conditions under which a classical solution or a Born approximation solution for differential cross section is valid have been given by Williams,<sup>6</sup> Bohr,<sup>5</sup> Mott and Massey,<sup>7</sup> and Firsov<sup>2</sup> as well as reference I. In regions where  $b/\lambda \ll 1$  the Born approximation solution is valid for all angles and the classical solution is nowhere valid. In regions where  $b/\lambda \gg 1$ , and also  $a/\lambda \gg 1$ , the classical solution is valid at angles much greater than a certain limiting angle

$\theta_c$  and the Born approximation solution is valid at angles much smaller than a limiting angle  $\theta_b$ .

It is necessary to develop formulas for  $\theta_c$  and  $\theta_b$  for the particular potential of Eq. (1) and to discuss the difficulties in integrating across the transition region.

The classical limiting angle  $\theta_c$  is found by requiring<sup>5-7</sup> that the collision be well defined within the limitations of the uncertainty principle  $\Delta p \Delta x \simeq \hbar$ . For small-angle collisions, the change in momentum  $\Delta p$  is  $m v \theta_c$ , or  $\hbar \theta_c / \lambda$ . A reasonable choice for the significant length  $\Delta x$  would be the impact parameter, or, more precisely, the classical distance  $r_0$  of closest actual approach during the collision in question. Substituting these into the above uncertainty relation leads to

$$\theta_c \simeq \lambda / r_0. \quad (5)$$

This is the same result which Mott and Massey show.<sup>7</sup> Their formula shows  $\lambda/a$ , but their  $a$  is identified with the significant scattering distance and is not to be confused with  $a$  used here as the screening radius. In fact the screening radius is very often several times smaller than  $r_0$  at the very small angles where the uncertainty limit applies.

The relationship between  $r_0$  and  $\theta$  is given<sup>8</sup> for small angles by

$$\theta a / b = K_1(r_0/a), \quad (6)$$

where  $K_1$  is the first order modified Bessel function of the second kind.

The desired upper limit  $\theta_b$  for the Born approximation solution is found from considerations discussed by Mott and Massey relating the potential energy at the distance  $\lambda/\theta$  with the scattering angle  $\theta$ . This relationship<sup>9</sup> is

$$V(\lambda/\theta_b) = m v^2 \theta_b. \quad (7)$$

Substituting the potential energy function of Eq. (1) into Eq. (7) the result can be written

$$\theta_b a / b = (\lambda/b) / [\ln(b/2\lambda)]. \quad (8)$$

This form is chosen in order to express the limit  $\theta_b$  in terms of the single parameter  $b/\lambda$ . The formula applies when  $b/\lambda$  is large, since for small  $b/\lambda$  the Born approximation solution is valid for all angles.

A third angle of interest is  $\theta'$ , that at which the classical and the Born approximation values of the differential cross section intersect. This angle is always less than both  $\theta_c$  and  $\theta_b$  and is very much less for large  $b/\lambda$ .

A typical case, that for  $b/\lambda = 5$  and  $b/a = 2$  is plotted in Fig. 1. This shows differential cross section computed with both classical and Born approximation formulas plotted vs angle of scattering and illustrates the three

<sup>4</sup> H. S. W. Massey and E. H. S. Burhop, *Electronic and Ionic Impact Phenomena* (Oxford University Press, New York, 1952), p. 367 ff.

<sup>5</sup> N. Bohr, Kgl. Danske Videnskab. Selskab, Mat.-fys. Medd. 18, 8 (1948).

<sup>6</sup> E. J. Williams, *Revs. Modern Phys.* 17, 217 (1945).

<sup>7</sup> N. F. Mott and H. S. W. Massey, *Theory of Atomic Collisions* (Oxford University Press, New York, 1949), 2nd ed., Chap. VII, Secs. 4 and 5.

<sup>8</sup> This analytic solution to Eq. (17) of reference I was pointed out by John L. Carter, Jr., in a private communication.

<sup>9</sup> N. F. Mott and H. S. W. Massey, reference 7. Their strong inequality at the top of p. 126 becomes our Eq. (7) when  $\theta$  is replaced by its limiting angle  $\theta_b$ .

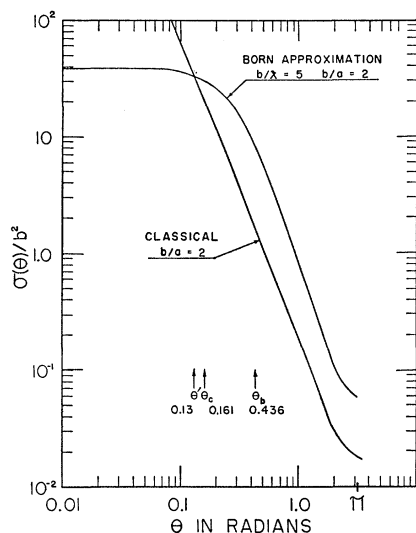


FIG. 1. A comparison of the classical and the Born approximation solutions for the differential cross section for scattering from a screened Coulomb potential energy function. It is drawn for the case  $b/\lambda = 5$  and  $b/a = 2$ . The classical solution is valid for angles much greater than  $\theta_c$  whereas the Born approximation solution is valid for angles much less than  $\theta_b$ . The curves intersect at angle  $\theta'$ .

angles  $\theta_c$ ,  $\theta_b$ , and  $\theta'$ . Other comparative values of these angles are given in Table I for various values of  $b/\lambda$ .

Figure 1 illustrates the difficulty encountered when computing total cross sections. On the one hand the classical solution is valid where  $\theta \gg \theta_c$  and the other solution is valid where  $\theta \ll \theta_b$ . It happens that  $\theta_c < \theta_b$  and there is some overlap, but the curves do not agree very well in the region where they overlap. Unfortunately there is no exact solution known, and no progress will be made unless one arbitrarily extends one or both curves into a region where the above strong inequalities are violated. There are two quite

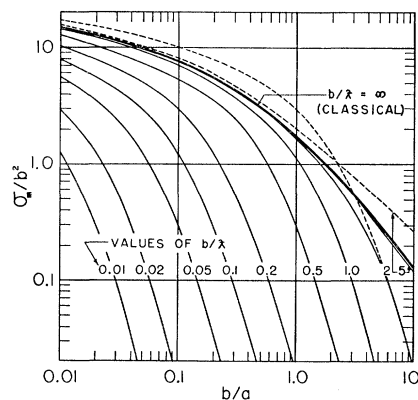


FIG. 2. Momentum transfer cross sections for a screened Coulomb potential energy function. Above  $b/\lambda = 1$  the results depend on the particular angle at which the change over is made from the classical to the Born approximation solution. The solid lines have  $\theta_c$  and the dotted lines have  $\theta_b$  as the "change over" angle.

arbitrary procedures. The first procedure would use the classical solution for angles greater than  $\theta_c$  and the other solution for all smaller angles. The second procedure would use the classical solution for angles greater than  $\theta_b$  and the other solution for smaller angles.

The two procedures give values for the total cross section computed in Sec. 4 which differ from each other by a factor of two for some values of  $b/\lambda$ . In view of the uncertain validity of either formula in the transition region both values are given. Accurate values of total cross section in these regions must await an exact solution for differential cross section.

There is one region, that for  $b/\lambda > 1$  and  $r_0/\lambda < 1$ , where there is a gap. Here the classical solution is nowhere valid and the Born approximation solution is good only at small angles. A discussion of this region is given by Bohr<sup>5</sup> who found justification for extending the Born approximation solution to partially close this gap.

TABLE I. Certain transition angles are given as a function of  $b/\lambda$ . Here  $\theta_c$  is the lower limit of validity of the classical solution,  $\theta_b$  is the upper limit of the Born approximation solution, and  $\theta'$  is the angle at which the two solutions intersect. The table is obtained using formulas valid at small angles.

$b/\lambda$	$\theta_c a/b$	$\theta_b a/b$	$\theta' a/b$
2	$4.06 \times 10^{-1}$	$\infty$	$3.7 \times 10^{-1}$
5	$8.33 \times 10^{-2}$	$2.18 \times 10^{-1}$	$6.6 \times 10^{-2}$
10	$3.11 \times 10^{-2}$	$6.22 \times 10^{-2}$	$1.87 \times 10^{-2}$
20	$1.25 \times 10^{-2}$	$2.17 \times 10^{-2}$	$5.3 \times 10^{-3}$
50	$3.99 \times 10^{-3}$	$6.21 \times 10^{-3}$	$9.7 \times 10^{-4}$
100	$1.74 \times 10^{-3}$	$2.56 \times 10^{-3}$	$2.7 \times 10^{-4}$
200	$7.72 \times 10^{-4}$	$1.03 \times 10^{-3}$	$7.4 \times 10^{-5}$
500	$2.67 \times 10^{-4}$	$3.62 \times 10^{-4}$	$1.24 \times 10^{-5}$
1000	$1.21 \times 10^{-4}$	$1.61 \times 10^{-4}$	$3.3 \times 10^{-6}$

### 3. MOMENTUM TRANSFER CROSS SECTION

The momentum transfer cross section  $\sigma_m$  is the sum of two terms

$$\sigma_m/b^2 = M_1 + M_2, \quad (9)$$

where  $M_1$  is the contribution from the region of small angles where the Born approximation applies and  $M_2$  is from the region where the classical solution is valid. Here

$$M_1 = 2\pi \int_0^{\theta_c} [\sigma(\theta)/b^2] (1 - \cos\theta) \sin\theta d\theta, \quad (10)$$

where the differential scattering cross section  $\sigma(\theta)$  is given by the well-known<sup>10</sup> formula

$$\begin{aligned} \sigma(\theta)/b^2 &= (a/\lambda)^4 / (L^2 a^2 + 1), \\ L &= (2a/\lambda) \sin(\theta/2). \end{aligned} \quad (11)$$

<sup>10</sup> See, for example, L. I. Schiff, *Quantum Mechanics* (McGraw-Hill Book Company, Inc., New York, 1949), p. 168.

Equation (10) is integrated to give

$$M_1 = (\pi/2)[\ln(L_c^2 a^2 + 1) - L_c^2 a^2 / (L_c^2 a^2 + 1)], \quad (12)$$

where  $L_c$  corresponds to the limiting angle  $\theta_c$ .

The second term in Eq. (9) is

$$M_2 = 2\pi \int_{\theta_c}^{\pi} [\sigma(\theta)/b^2] (1 - \cos\theta) \sin\theta d\theta. \quad (13)$$

This was evaluated numerically using the classical values of differential cross section from reference I.

Although  $\theta_c$  has been taken as the transition angle in Eqs. (10)–(13), the calculations were repeated using  $\theta_b$ . The resulting values of momentum transfer cross section are shown in Fig. 2. The solid curves were calculated using  $\theta_c$  and those calculated using  $\theta_b$  are shown dotted where they differ appreciably.

A transition occurs at  $b/\lambda$  equal to about two. Below this line the Born approximation solution applies at all angles. Here  $M_2=0$  and  $\theta_c$  is replaced by  $\pi$  in Eqs. (10) and (12). For  $b/\lambda > 2$  there are contributions from both  $M_1$  and  $M_2$ . The discrepancy between solid and

TABLE II. Classical values of the momentum transfer cross section for the screened Coulomb potential energy function. Here  $b/\lambda = \infty$ .

$b/a$	$\sigma_m/b^2$	$b/a$	$\sigma_m/b^2$
10	0.125	0.2	5.58
5	0.309	0.1	7.78
2	0.889	0.05	9.89
1	1.76	0.02	12.9
0.5	3.10	0.01	15.2

dotted curves illustrates the effect of the choice of transition angle and shows the need for an exact solution.

The limiting case,  $b/\lambda = \infty$ , is of particular interest since this corresponds to an entirely classical solution. In this case  $M_1$  is zero and the integration of  $M_2$  extends from 0 to  $\pi$ . The momentum transfer cross section is finite, and is a function of  $b/a$  alone. In the unscreened case of Rutherford scattering, where  $a \rightarrow \infty$  and  $b/a \rightarrow 0$ , the momentum transfer cross section is infinite. Figure 2 shows, however, that a slight amount of screening suffices to insure a finite value. Classical values of  $\sigma_m/b^2$  are given in Table II.

The solid and dotted curves for  $b/\lambda = 2$  in Fig. 2 lie on either side of the limiting curve  $b/\lambda = \infty$ , and all curves for  $b/\lambda > 2$  lie clustered in this same vicinity. This situation comes about because the Born approximation differential cross section of Eq. (11) lies considerably above the corresponding classical differential cross section of reference I at medium to large angles. As  $b/\lambda$  increases the transition angle decreases in such a way that the curves for  $b/\lambda$  in excess of two are all practically coincident with the limiting case  $b/\lambda = \infty$ .

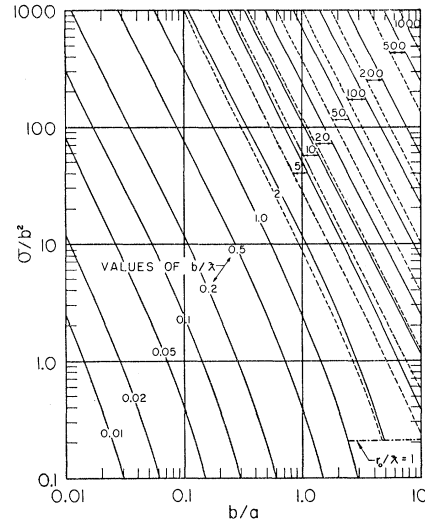


FIG. 3. Total cross sections for scattering from a screened Coulomb potential energy function. The solid lines have  $\theta_c$  and the dotted lines have  $\theta_b$  as the "change over" angle. At the upper and left edges of the figure all lines have slope  $-2$  on log log paper and may be extended without limit.

#### 4. TOTAL CROSS SECTION

The total scattering cross section  $\sigma$  is also the sum of two terms

$$\sigma/b^2 = I_1 + I_2, \quad (14)$$

where

$$I_1 = 2\pi \int_0^{\theta_c} [\sigma(\theta)/b^2] \sin\theta d\theta, \quad (15)$$

$$I_2 = 2\pi \int_{\theta_c}^{\pi} [\sigma(\theta)/b^2] \sin\theta d\theta.$$

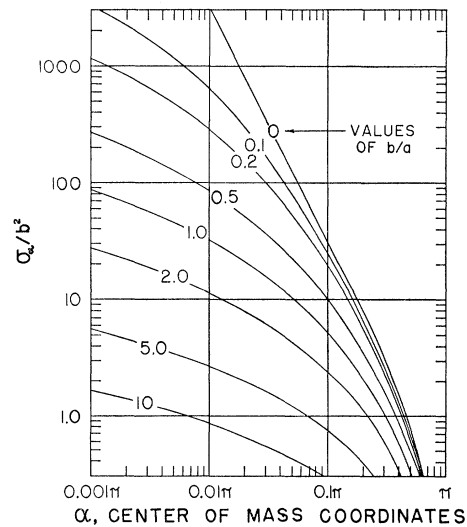


FIG. 4. Limited classical total cross section for scattering from a screened Coulomb potential energy function. Only those particles are included which are scattered to angles in excess of the specified angle  $\alpha$ .

The first of these is readily integrated using Eq. (11), and the second term equals  $\pi(p_c/b)^2$  where  $p_c$  is the classical impact parameter corresponding to  $\theta_c$  as tabulated in reference I. The result is

$$\sigma/b^2 = (\pi a^2/\lambda^2) L_c^2 a^2 / (L_c^2 a^2 + 1) + \pi(p_c/b)^2. \quad (16)$$

For  $b/\lambda \leq 1$  the total cross section is given entirely by extending  $I_1$  from 0 to  $\pi$ , and the well-known result is

$$\sigma/b^2 = (4\pi a^4/\lambda^4)/(1+4a^2/\lambda^2). \quad (17)$$

The total cross sections are shown in Fig. 3. The solid lines are those in which  $\theta_c$  was chosen as the transition angle, and the dotted lines have  $\theta_b$  as the transition angle. At the top and the left edge of the figure all lines have slopes  $-2$  on log log paper and may be extended without limit.

### 5. LIMITED TOTAL CROSS SECTION

The limited total cross section  $\sigma_\alpha$  is defined here as the cross section for scattering to angles in excess of a

specified angle  $\alpha$ . Experimental measurements of scattering cross sections must have a lower angular limit because of the finite angular resolution of the apparatus and the impossibility of differentiating between an unscattered particle and one which has been scattered through a negligible angle.

A study of Table I shows that  $\theta_c$  and  $\theta_b$  are very small angles, much less than one degree for large values of  $b/\lambda$ . Thus the classical solution is often valid for angular regions which can be measured experimentally.

The limited total cross section is found very simply from

$$\sigma_\alpha = \pi p_\alpha^2, \quad (18)$$

where  $p_\alpha$  is the classical impact parameter corresponding to scattering through an angle  $\alpha$  as found in reference I. For convenience in comparison with experiments Fig. 4 plots values of this cross section as it depends on  $b/a$  and the specified angle  $\alpha$ .

## Efficiency of Field Ionization at a Metal Surface

H. FIEDELDEY\* AND D. FOURIE

*Physics Department, University of Pretoria, Pretoria, South Africa*

(Received September 1, 1959)

In this paper the expression for the transmission coefficient, which was derived formerly by Müller for field emission, is integrated by making certain approximations. The formula for the efficiency of field ionization could then be integrated. Furthermore the supply function is calculated by regarding the molecule as moving in a central field of force. The main object of the paper is that of deriving analytical formulas which give a better picture of the dependence of the field ion current on the various parameters.

### 1. INTRODUCTION

MÜLLER<sup>1</sup> has shown that, in a field up to  $500 \times 10^6$  volts/cm, the mechanism by which field emission of positive ions takes place in the field ion microscope depends upon the supply of molecules and their field ionization probability.

As the molecule approaches the tip from the low-field region where the ionization is negligible, to the high-field region near the tip, the ionization will increase due to a reduction in height and breadth of the potential wall which binds the electron and will reach a sharp limit when the ground level of the molecule sinks below the Fermi level of the emitter.

Müller<sup>1,2</sup> has calculated the ionization probability for a molecule approaching the tip from a distance  $L$  A up to  $(L-1)$  A with a speed depending on the field  $F$

and the molecular polarizability. He has taken the effective potential of the escaping electron to be

$$V(x) = \frac{-e}{L-x} + Fx - \frac{e}{4x} + \frac{e}{L+x}, \quad (1)$$

in a one-dimensional approximation of the problem. The terms on the right are, respectively, associated with the Coulomb attraction between ion and electron, the applied field, the image of the electron in the metal (tip) surface and the image of the ion. A wave mechanical calculation leads to the formula

$$D(L) = \exp \left\{ - \left( \frac{8em}{\hbar^2} \right)^{\frac{1}{2}} \int_{x_1}^{x_2} \left[ V(x) - FL + V_I - \frac{e}{4L} \right]^{\frac{1}{2}} dx \right\} \quad (2)$$

for the penetration probability of the electrons where  $V_I$  is the ionization potential.

In a rough approximation for the three dimensional

\* For this investigation, H. Fiedeldey received a bursary from the Council for Scientific Industrial Research, Pretoria.

<sup>1</sup> E. W. Müller and K. Bahadur, *Phys. Rev.* **102**, 624 (1956).

<sup>2</sup> R. H. Good and E. W. Müller, *Encyclopedia of Physics* (Springer-Verlag, Berlin, 1956), Vol. 21.